

Surface plasmon resonance modulation in nanopatterned Au gratings by the insulator-metal transition in vanadium dioxide films

M. Beebe,^{1,*} L. Wang,¹ S. E. Madaras,¹ J. M. Klopff,¹ Z. Li,¹ D. Brantley,¹ M. Heimburger,¹ R. A. Wincheski,² S. Kittiwatanakul,³ J. Lu,³ S. A. Wolf,^{3,4} and R. A. Lukaszew¹

¹Department of Physics, College of William and Mary, Williamsburg, Virginia 23187, USA

²NASA Langley Research Center, Hampton, Virginia 23681, USA

³Department of Material Sciences and Engineering, University of Virginia, Charlottesville, Virginia 22904, USA

⁴Department of Physics, University of Virginia, Charlottesville, Virginia 22904, USA

*mrbeebe@email.wm.edu

Abstract: Correlated experimental and simulation studies on the modulation of Surface Plasmon Polaritons (SPP) in Au/VO₂ bilayers are presented. The modification of the SPP wave vector by the thermally-induced insulator-to-metal phase transition (IMT) in VO₂ was investigated by measuring the optical reflectivity of the sample. Reflectivity changes are observed for VO₂ when transitioning between the insulating and metallic states, enabling modulation of the SPP in the Au layer by the thermally induced IMT in the VO₂ layer. Since the IMT can also be optically induced using ultrafast laser pulses, we postulate the viability of SPP ultrafast modulation for sensing or control.

©2015 Optical Society of America

OCIS codes: (050.2770) Gratings; (240.0310) Thin films; (240.6680) Surface plasmons; (310.6860) Thin films, optical properties; (310.6628) Subwavelength structures, nanostructures; (310.6845) Thin film devices and applications.

References and links

1. N. I. Zheludev and Y. S. Kivshar, "From metamaterials to metadevices," *Nat. Mater.* **11**(11), 917–924 (2012).
2. L. Wang, K. Yang, C. Clavero, A. J. Nelson, K. J. Carroll, E. E. Carpenter, and R. A. Lukaszew, "Localized surface plasmon resonance enhanced magneto-optical activity in core-shell Fe-Ag nanoparticles," *J. Appl. Phys.* **107**, 09B303 (2010).
3. X. Huang, I. H. El-Sayed, W. Qian, and M. A. El-Sayed, "Cancer cell imaging and photothermal therapy in the near-infrared region by using Gold nanorods," *J. Am. Chem. Soc.* **128**(6), 2115–2120 (2006).
4. W. L. Barnes, A. Dereux, and T. W. Ebbesen, "Surface plasmon subwavelength optics," *Nature* **424**(6950), 824–830 (2003).
5. A. Cavalleri, C. Tóth, C. W. Siders, J. A. Squier, F. Ráksi, P. Forget, and J. C. Kieffer, "Femtosecond structural dynamics in VO₂ during an ultrafast solid-solid phase transition," *Phys. Rev. Lett.* **87**(23), 237401 (2001).
6. F. J. Morin, "Oxides which show a metal-to-insulator transition at the Neel temperature," *Phys. Rev. Lett.* **3**(1), 34–36 (1959).
7. S. Kittiwatanakul, J. Laverock, D. Newby, K. E. Smith, S. A. Wolf, and J. Lu, "Transport behavior and electronic structure of phase pure VO₂ thin films grown on c-plane sapphire under different O₂ partial pressure," *J. Appl. Phys.* **114**(5), 053703 (2013).
8. S. Lysenko, A. Rúa, V. Vikhnin, F. Fernández, and H. Liu, "Insulator-to-metal phase transition and recovery processes in VO₂ thin films after femtosecond laser excitation," *Phys. Rev. B* **76**(3), 035104 (2007).
9. M. Rini, Z. Hao, R. W. Schoenlein, C. Giannetti, F. Parmigiani, S. Fourmaux, J. C. Kieffer, A. Fujimori, M. Onoda, S. Wall, and A. Cavalleri, "Optical switching in VO₂ films by below-gap excitation," *Appl. Phys. Lett.* **92**(18), 181904 (2008).
10. B. Wang and G. P. Wang, "Plasmon Bragg reflectors and nanocavities on flat metallic surfaces," *Appl. Phys. Lett.* **87**(1), 013107 (2005).
11. H. Raether, *Surface Plasmons on Smooth and Rough Surfaces and on Gratings* (Springer-Verlag, 1986).
12. J. Nag, "The solid-solid phase transition in vanadium dioxide thin films: synthesis, physics and application," Ph.D. thesis (Vanderbilt, Nashville, TN, 2011).
13. J. Y. Suh, E. U. Donev, R. Lopez, L. C. Feldman, and R. F. Haglund, "Modulated optical transmission of subwavelength hole arrays in metal-VO₂ films," *Appl. Phys. Lett.* **88**(13), 133115 (2006).

14. M. J. Dicken, K. Aydin, I. M. Pryce, L. A. Sweatlock, E. M. Boyd, S. Walavalkar, J. Ma, and H. A. Atwater, "Frequency tunable near-infrared metamaterials based on VO₂ phase transition," *Opt. Express* **17**(20), 18330–18339 (2009).
15. K. G. West, J. Lu, J. Yu, D. Kirkwood, W. Chen, Y. Pei, J. Claassen, and S. A. Wolf, "Growth and characterization of vanadium dioxide thin films prepared by reactive-biased target ion beam deposition," *J. Vac. Sci. Technol. A* **26**(1), 133–139 (2008).
16. L. Wang, E. Radue, S. Kittiwatanakul, C. Clavero, J. Lu, S. A. Wolf, I. Novikova, and R. A. Lukaszew, "Surface plasmon polaritons in VO₂ thin films for tunable low-loss plasmonic applications," *Opt. Lett.* **37**(20), 4335–4337 (2012).
17. E. Radue, E. Crisman, L. Wang, S. Kittiwatanakul, J. Lu, S. A. Wolf, R. Wincheski, R. A. Lukaszew, and I. Novikova, "Effect of a substrate-induced microstructure on the optical properties of the insulator-metal transition temperature in VO₂ thin films," *J. Appl. Phys.* **113**(23), 233104 (2013).
18. Grating Solver Development Co., retrieved <http://www.gsolver.com/>.
19. E. D. Palik, *Handbook of Optical Constants of Solids* (Academic, 1998).
20. H. W. Verleur, A. S. Barker, and C. N. Berglund, "Optical properties of VO₂ between 0.25 and 5 eV," *Phys. Rev.* **172**(3), 788–798 (1968).

1. Introduction

Current interest in SPP technology is focused on the development of nanoscale optical devices to control the propagation of light in sub-wavelength geometries [1–4]. The use of photons and electrons together in such technologies is desirable for developing opto-electronic protocols to speed up information processing and transmission, as well as for biological sensing and new imaging techniques. There are a number of materials and structures with unique properties that can be exploited for these applications, including vanadium dioxide (VO₂). VO₂ is well-known as a material exhibiting an insulator-to-metal phase transition (IMT) that can be optically [5], thermally [6], and electrically [7] induced, and optical switches using VO₂ have gained attention due to their extremely fast switching speeds (<100 fs) [8] and very low switching energies (on the order of 1 pJ/μm²) [9]. In all-optical devices, SPPs enhance the local optical field intensity in the region of sub-wavelength structures [10], producing a strong non-linear effect, thus allowing for new ways to control light propagation. As such, it is of interest to combine these plasmonic effects with the optical transition of VO₂.

When exciting SPPs using only light, the wave vector of the incident light is smaller than that needed to excite the SPPs, *i.e.* $k_i < k_{sp}$, where $k_i = k_0 \sin\theta$ is the in-plane wave vector of incident light in vacuum, $k_{||} = \omega/c$, and θ is the incident angle. The dispersion relations of the incident light and the SPPs are shown in Fig. 1(a). To overcome the difference in wave vectors, $k_{||}$ can be increased to match k_{sp} by using optical couplers such as a prism in the so-called Kretschmann configuration or by using diffraction gratings [11]. In the latter case, $k_{||}$ can be enhanced to match k_{sp} by adding integer multiples of a grating wave vector \mathbf{g} as $k_{sp} = k_{||} + m\mathbf{g} = k_0 \sin\theta$ (1), where $\mathbf{g} = 2\pi/a$, m is an integer representing the diffraction order, and a is the pitch of the grating. The SPP is observed as a sharp minimum in the $m = 0$ order reflection when the angle of incidence satisfies Eq. (1). Note that in this equation all three vectors – $k_{||}$, k_{sp} , and \mathbf{g} – must be collinear; the direction of the grating grooves must be perpendicular to the plane of incidence and the illuminating light must be *p*-polarized (Fig. 1(b)) This is the configuration that we used in the experiments presented here. If instead the direction of the grating grooves is at an angle $\psi \neq 90^\circ$ with respect to the plane of incidence, then the above equation should be replaced by a ψ -dependent equation, and, under certain condition, *s*-polarized light can also excite the SPPs [12].

Although combinations of nanostructured noble metals and VO₂ layers have been studied and reported in recent times [13, 14], here we present the first correlated experimental investigation and simulations of SPPs on Au gratings patterned onto a VO₂ thin film thus enabling tailoring such structures for greatest benefit.

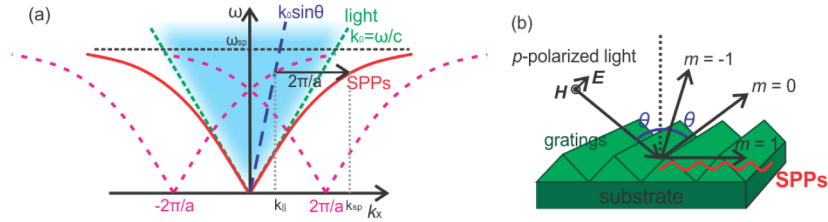


Fig. 1. (a) The dispersion relation curves corresponding to light in vacuum (green dashed lines) and SPPs (solid red lines). Pink dashed lines represent the SPP curves offset by $2\pi/a$. The shaded region is bounded by light lines representing the area in which SPPs can be excited. (b) Schematic of the SPP excitation on gratings. The plane of incidence is perpendicular to the direction of grating grooves.

2. Experimental procedure

2.1 Sample structure

The crystalline VO_2 thin films studied were ~ 70 nm thick and grown on quartz using reactive based target ion beam deposition [15]. The surface morphology and crystalline structure of these films have been previously characterized and discussed elsewhere [16].

Temperature-dependent infrared (IR) optical transmission studies showed a significant transmission decrease from the room temperature (RT) insulating state to the high temperature (340 K) metallic state, showing the thermally induced IMT of the VO_2 films [15]. A 65 nm Au layer was then evaporated onto the VO_2 film and e-beam lithography was used to pattern a diffraction grating on the Au surface, with the grooves piercing through the Au layer so that optical transmission measurements would be possible. Atomic force microscopy (AFM), shown in Figs. 2(a) and 2(c), was carried out to characterize the morphology of the Au gratings. The gratings were found to have a width of approximately 400 nm and a pitch of 2.5 μm . In addition, line scans were performed along the grating vector direction (green lines) to provide more detailed information about the gratings, shown in Figs. 2(b) and 2(d). These scans showed an additional structure at the edges of the rectangular grooves, which previous experience indicates is likely due to residual Au material remaining along the edge of the grooves after the lift-off step of the lithography process, as demonstrated in Fig. 3(a). AFM scans in multiple directions show this residual Au, evidence that the structure is real and not simply due to AFM tip overshoot; a schematic of the sample structure is shown in Fig. 3(b). In our simulations, we considered rectangular grooves both with and without the added Au structures.

2.2 Experimental setup

The experimental setup described here and shown in Fig. 4(a) was used to investigate the effect of the thermally-induced IMT of VO_2 on the SPP excitation of the Au gratings. The film was mounted on a pierced thermoelectric cooler (TEC) stage to allow for temperature-dependent measurements and to allow both IR reflectivity and transmission measurements. The sample on the TEC was then mounted on a custom-built goniometer system such that the grating vector was parallel to the plane of incidence. The goniometer stage was computer-controlled to measure the sample's reflectivity as a function of the incident angle with 0.01° resolution. A p -polarized red He-Ne laser ($\lambda = 632$ nm) modulated with a 503 Hz optical chopper mounted on one arm of the goniometer illuminated the sample grating over a range of incident angles. A glass window was used to pick off a fraction of the incident laser beam so that the incident power could be monitored throughout the experiment; Si photodetectors and lock-in amplifiers were used to measure both this reference beam and the reflected beam. The sample stage was carefully aligned, bringing the grating surface into coincidence with the stage's axis of rotation so that the incident beam did not move on the sample surface as the incident angle was varied. In addition to the reflectance measurements, we performed IR

transmission measurements using an IR He-Ne laser ($\lambda = 1520 \text{ nm}$) at normal incidence. The transmitted intensity was measured using a Ge photodetector with an IR filter. The sample was kept at a constant temperature using the TEC as the red laser light was stepped through a range of angles; once this sweep was done, the temperature was increased and the process was repeated for each new temperature.

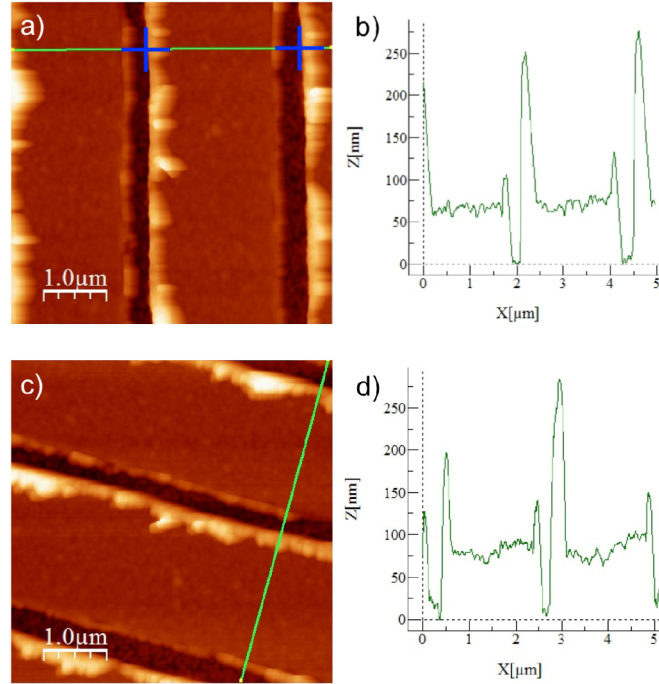


Fig. 2. (a) AFM topography image of the Au gratings. Green lines indicate line scans along the grating vector direction. The two blue crosses show one grating period along a line scan. (b) A line profile extracted from the AFM line scans. (c) AFM topography and (d) a line profile of the gratings in an additional direction.

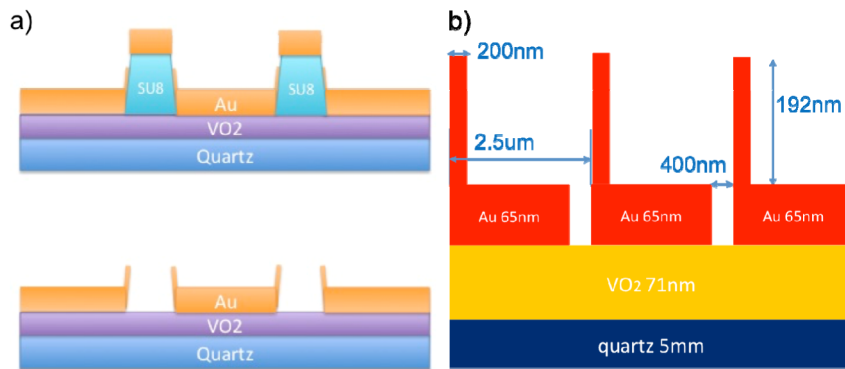


Fig. 3. (a) The lift-off step in the lithography process, which caused the additional Au structures seen in the AFM line scans in Figs. 2(b) and 2(d). (b) A schematic of the sample structure as determined by AFM.

2.3 Measurements

As discussed above, temperature-dependent IR transmission of the VO₂ film was measured through the Au gratings grooves at normal incidence in order to determine the IMT properties of the film, as shown in Fig. 5 (left axis). A significant IR transmission decrease takes place during the IMT, indicating that the deposition and etching of the Au did not significantly affect the thermally-induced IMT properties of the VO₂, although the transition temperature was observed to be slightly lower than the well-known value of 340 K. This is mainly due to the strain inherent in thin film crystalline structures as reported elsewhere [17].

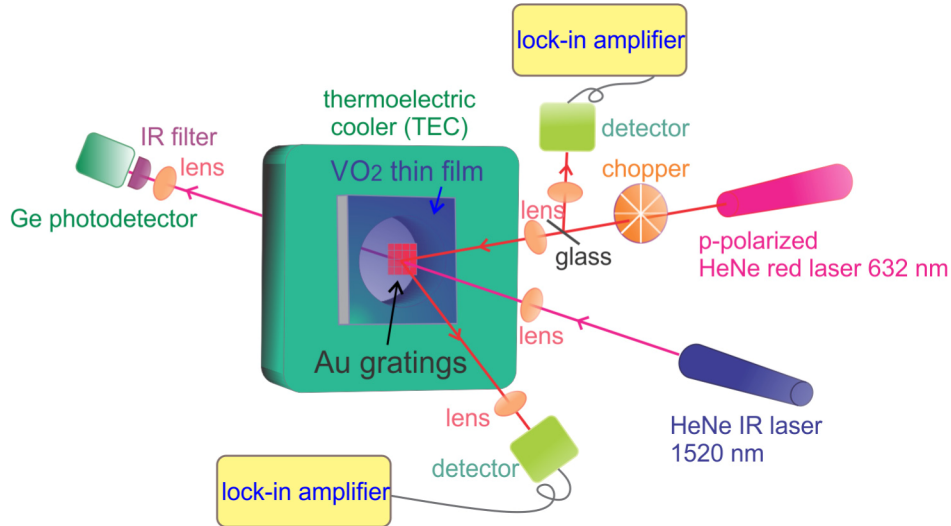


Fig. 4. (a) Schematic of the experimental setup for temperature-dependent red SPP and IR transmission measurements of a Au grating on VO₂ thin film.

Also plotted in Fig. 5 (right axis), the reflectance of the red laser from the Au grating at a fixed incident angle was measured as a function of temperature. The incident angle was scanned over a range of angles around the SPP excitation angle (also referred to as the critical angle θ_c , determined to be $\theta_c = 44.75^\circ$). It is worth noting that the reflection of the red laser from the Au gratings shows a similar decrease as the IR transmission of the VO₂ during the IMT, which indicates that the SPP excitation on the Au gratings is modulated by the IMT in the VO₂.

To study this change in the SPP properties of the Au gratings under the VO₂ IMT, the reflection of the red laser was measured as a function of incident angle and temperature. The experimental results are shown in Fig. 6(a). The reflection was measured with the VO₂ in both the insulating state ($T = 303$ K) and the metallic state ($T = 331$ K), indicated by the two stars in the IR transmission curve in Fig. 5. To confirm the SPP resonance angle θ_c , which occurs around 45° based on simulations, we first used the sample stage goniometer to measure reflection through a wide angular spectrum from 20° to 75° at RT. Precision measurements were then taken from 42° to 47° , where, as seen in Fig. 6(a), a reflection minimum evidencing an SPP resonance occurred at $\theta_c = 44.75^\circ$ due to the SPP excitation on the Au gratings. We have carried out preliminary studies on transmission and reflection geometries in thin Au and Ag films deposited on gratings, confirming that these precision measurements show a surface plasmon resonance absorption at 44.75° . The resonance was seen at 44.75° at both $T = 303$ K and $T = 331$ K, although it is clear that the SPP resonance is stronger when the VO₂ is in the metallic state ($T = 331$ K).

3. Simulations

The optical response in this thin film/grating structure was simulated using the GSolver grating simulation software [18], which describes the reflection of light from a periodic grating structure by solving Maxwell's equations using a class of algorithms known as Rigorous Coupled Wave (RCW) analysis. In our simulations, the sample's structure was simulated using rectangular shaped Au gratings first without and then with additional Au structures at one end on top of a continuous layer of VO₂. The optical properties for the sample layers were applied to the simulations using constant optical properties for the Au layer ($n = 0.1984$, $k = 3.0875$) [19], while using optical properties for the VO₂ layer in the insulating ($n = 2.85$, $k = 0.341771$) and metallic ($n = 2.22$, $k = 0.600000$) states based on measurements of similar VO₂ thin films [20]. The results from both simulations are shown in Figs. 7(a) and 7(b) for comparison, although only the simulation with the added Au structure (Fig. 7(b)) is used.

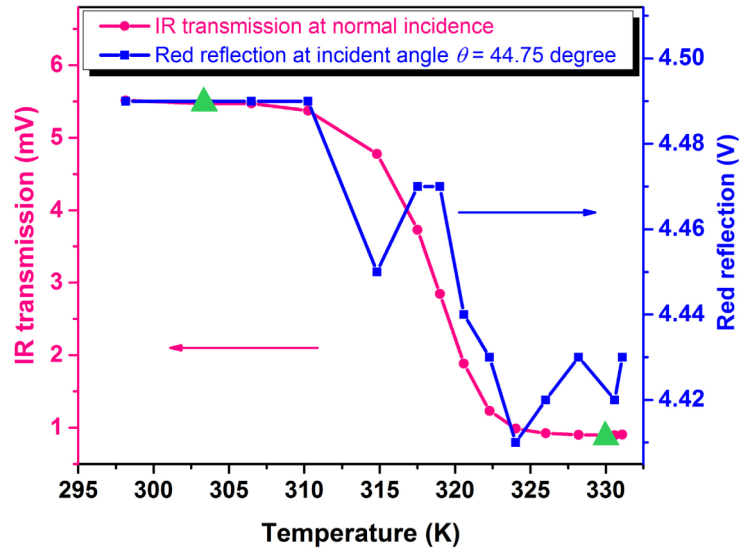


Fig. 5. The IR transmission ($\lambda = 1520$ nm) of the VO₂ thin film at normal incidence (left axis) and the red reflection ($\lambda = 632$ nm) of the Au gratings at the SPP critical angle $\theta_c = 44.75^\circ$ (right axis) as a function of temperature. The two triangles indicate the temperature at which the detailed angular measurements were taken in Fig. 6(a), with the VO₂ in the insulating state ($T = 303$ K) and the metallic state ($T = 331$ K).

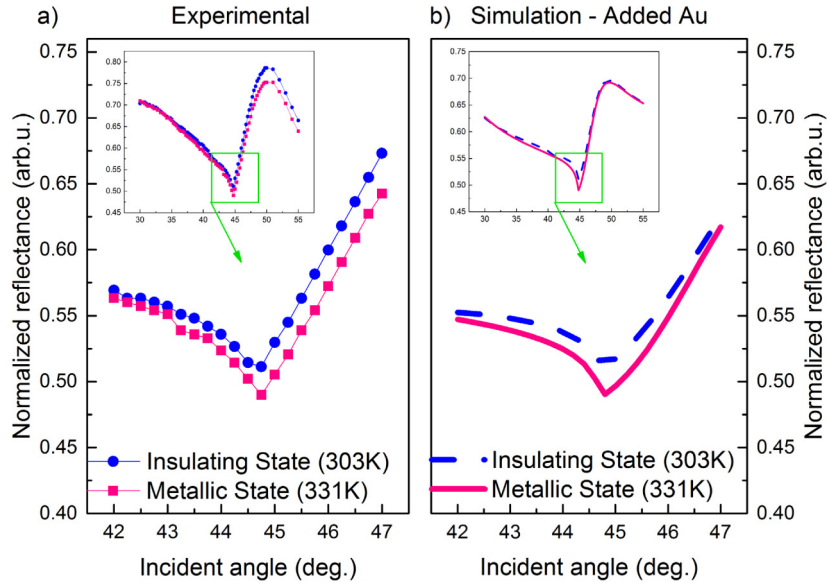


Fig. 6. Experimental (a) and simulated (b) reflectance of Au gratings on a VO₂ thin film as a function of incident angle at two different temperatures correspondent to VO₂ in the insulating state (T = 303 K) and metallic state (T = 331 K). The inset figures in (a) and (b) show the full wide range plot of the experimental and simulated reflectance. Both the experiment and simulation were performed at 632nm.

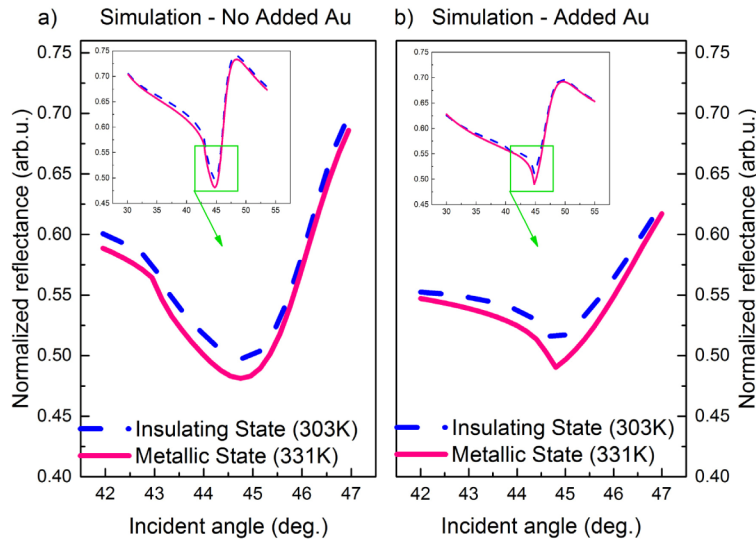


Fig. 7. Simulated reflectance of Au gratings (a) without and (b) with additional Au structures at 632nm. The inset figures in (a) and (b) show the full wide range plot of the simulated reflectance.

The results of the simulations used are also displayed in Fig. 6(b), and it can be seen that there is very good agreement between the simulation and our experimental results. The simulations do show a slightly stronger effect than we see in our real sample; this may be due to the various processing steps used to create the diffraction pattern in the gold over-layer. Nevertheless, our simulations also indicate that the additional Au structure formed at the groove edges due to the lift-off process seems to enhance the effect compared to flat edges

showcasing a possible path for further enhancement via tailoring the design and the processing steps to create it.

4. Conclusion

In conclusion, we have studied the SPP excitation in an Au grating/ VO_2 thin film structure for potential photonic/plasmonic applications. We found that deposition and etching of the Au gratings did not degrade the quality of the thermally-induced IMT contrast in the VO_2 thin film. The reflectance measurements showed the SPP excitation in the Au gratings at $\theta_c = 44.75^\circ$ for both the low temperature insulating and high temperature metallic state of the VO_2 and that the Au SPP absorption resonance is made stronger when the VO_2 is transitioned to the high temperature metallic state, evidence that the SPP resonance is extremely sensitive to changes in the underlying layer. In addition, the optical reflectance simulations of the bi-layer grating structure are in excellent agreement with our experimental measurements. Our results demonstrate a method for tailoring the SPP modulation in the Au by the IMT in the underlying VO_2 film. These findings have broader impact when considering that the IMT in VO_2 can also be optically induced on a sub-picosecond timescale using ultrafast laser pulses [11], pointing to the great potential for an ultrafast SPP modulation scheme for all-optical detection and switching. This holds particular interest for defense applications involving optical limiters.

Acknowledgments

Aspects of this work were supported by a grant from the National Science Foundation (NSF-DMR-1006013) and by the Virginia Microelectronics Consortium (VMEC).